Internal localized eigenmodes on spin discrete breathers in antiferromagnetic chains with on-site easy-axis anisotropy

Sang Wook Kim[1] and Seunghwan Kim[2]

[1]*Max-Planck-Institut für Physik komplexer Systeme, Nöthnitzer Straße 38, D-01187 Dresden, Germany*

[2]*Asia Pacific Center for Theoretical Physics, Nonlinear and Complex Systems Laboratory, Department of Physics, Pohang University of Science and Technology, Pohang 790-784, Korea*

We investigate internal localized eigenmodes of the linearized equation around spin discrete breathers in one-dimensional antiferromagnets with on-site easy-axis anisotropy. The threshold of occurrence of the internal localized eigenmodes has a typical structure in the parameter space depending on the frequency of the spin discrete breather. We also performed molecular-dynamics simulation in order to show the validity of our linear analysis.

Discrete breathers (DB's) are the time-periodic and spatially localized excitations on the nonlinear lattice with translational invariance,[1,2] which are also called intrinsic localized modes in the literature.[3] The existence of DB's was mathematically proved in the anticontinuous limit.[4] Both the discreteness and the nonlinearity play a crucial role in the existence of DB's. The spatial discreteness is quite common in nature, particularly in condensed-matter physics. Recently, the experimental realization of a DB was performed in anisotropic antiferromagnets[5] and Josephson-junction ladders.[6]

In magnetic systems, both the spin-spin exchange interaction and the on-site spin anisotropy are intrinsically nonlinear, so that it is quite natural to predict the existence of DB's. Since the dissipation of spin waves in magnetic materials is usually weak compared with that of lattice vibrations in crystals, the spin-lattice model has obvious advantages over lattice vibrational models from the experimental points of view. Lai and Sievers have extensively studied the DB's of spin wave, namely spin DB's, for various situations of antiferromagnets.[7] The spin DB's have also been recently studied in ferromagnetic lattices.[8]

The DB can play a role of the scattering center affecting energy transport by scattering, absorbing, or radiating phonons. The scattering properties of the DB are closely related to the structure of the eigenmodes of the linearized equation around the DB itself,[9–12] which will be called *internal* localized eigenmodes (ILE's). In particular, it was shown that the perfect transmission occurs at the ILE threshold, where the ILE should appear to be tangent to the phonon band edge with the zero wave number in the angular frequency versus the system parameter space.[10,11] However, when the ILE's on DB's penetrate the phonon band, the well-known Fano resonances are obtained.[12] These results can be directly applied to the spin-lattice model considering the analogy between the lattice vibration (phonon) and the rotation of spin (magnon or spin wave).

In this paper, we present the existence of the ILE's on spin DB's using the linearized equation of spin DB's in one-dimensional (1D) antiferromagnets with on-site easy-axis anisotropy. The thresholds of the ILE's show some special structure in parameter space. The comparison between the prediction from linear analyses and the results of molecular-dynamics simulation will also be presented.

Let us consider an antiferromagnetic chain of N spins with the Hamiltonian[13]

$$H = 2J \sum_n \mathbf{S}_n \cdot \mathbf{S}_{n+1} - D \sum_n (S_n^z)^2, \quad (1)$$

where positive J and D are the exchange constant and the single-ion anisotropy constant, respectively. Hence, the antiferromagnetic ordering and aligning with z direction of each spin are energetically more favorable in the ground state.

For a nondissipative chain of classical spins, the equation of motion for the spin at the nth site is

$$\frac{d\mathbf{S}_n}{dt} = \mathbf{S}_n \times \mathbf{H}_n^{eff}, \quad (2)$$

where the effective field $\mathbf{H}_n^{eff}$ can be obtained from

$$\mathbf{H}_n^{eff} = -\boldsymbol{\nabla}_{\mathbf{S}_n} H = -2J(\mathbf{S}_{n-1} + \mathbf{S}_{n+1}) + 2D S_n^z \hat{\mathbf{z}}. \quad (3)$$

Here $\hat{\mathbf{z}}$ is the unit vector along the positive z direction. By using $s_n^{\pm} = (S_n^x \pm i S_n^y)/S$, the nonlinear equation of motion for s_n^+ can be obtained in the following:

$$i\hbar \frac{ds_n^+}{dt} = -2JS[(s_{n-1}^z + s_{n+1}^z)s_n^+ - (s_{n-1}^+ + s_{n+1}^+)s_n^z] + 2DS s_n^z s_n^+. \quad (4)$$

If we assume a solution of the form $s_n^+ = s_n e^{-i\omega t}$ and antiferromagnetic spin ordering, the stationary spin DB can be numerically obtained by using the following equation:

$$\tilde{\hbar}\omega s_n = (-1)^n \left\{ C\left(\sqrt{1 - s_{n-1}^2} + \sqrt{1 - s_{n+1}^2} \right) s_n + [C(s_{n-1} + s_{n+1}) + s_n] \sqrt{1 - s_n^2} \right\}, \quad (5)$$

where $\tilde{\hbar} = \hbar/2DS$ and $C = J/D$. In this paper we consider only a single nonmoving spin DB. The familiar dispersion

relation of the extended spin-wave modes, $\tilde{\hbar}\omega = \pm\sqrt{(1+2C)^2 - 4C^2\cos^2 ka}$, can also be obtained from Eq. (5) by putting

$$\begin{pmatrix} s_{2n} \\ s_{2n+1} \end{pmatrix} = \begin{pmatrix} f_0 e^{2ikna} \\ f_1 e^{ik(2n+1)a} \end{pmatrix}, \quad (6)$$

where a is the lattice spacing, and $|f_0|$, $|f_1| \ll 1$. The linearized equation of Eq. (4) near the spin DB for $\xi_n(t) = s_n^+(t) - s_n e^{-i\omega_b t}$ is given by

$$i\tilde{\hbar}\xi_n = (-1)^n \{ C[(A_{n-1} + A_{n+1})\xi_n - s_n(B_{n-1}\mathrm{Re}(\xi_{n-1}) $$
$$+ B_{n+1}\mathrm{Re}(\xi_{n+1})) + A_n(\xi_{n-1} + \xi_{n+1}) - B_n(s_{n-1} $$
$$+ s_{n+1})\mathrm{Re}(\xi_n)] + A_n\xi_n - s_n B_n\mathrm{Re}(\xi_n)\} - \tilde{\hbar}\omega_b\xi_n, $$
$$(7)$$

where $A_n = \sqrt{1 - s_n^2}$, $B_n = s_n/(2\sqrt{1 - s_n^2})$, and $\mathrm{Re}(\xi)$ is the real part of ξ. The above Floquet (or linear) equation is written in the form $d\vec{\xi}/dt = M\vec{\xi}$. By diagonalizing the matrix M, the eigenmodes for small perturbation of spin DB's are obtained. Let us note that there exist two important system parameters, the relative strength of the exchange interaction, C ($= J/D$), and the frequency of spin DB, ω_b.

Without the exchange interaction, i.e. $J = 0$, the resonance frequency of a local nonlinear oscillator is limited to $\omega_m = 1/\tilde{\hbar}$ since the nonlinearity of the individual system is soft. In the case $\omega_b/\omega_m > 1$, spin DB's cannot exist in the small coupling limit ($J \to 0$), so that we obtain two distinct regions for ω_b such as $\omega_b/\omega_m > 1$ and $\omega_b/\omega_m < 1$. In the former case ($\omega_b/\omega_m > 1$), the spin DB's can exist only above the certain critical value of C, which can be explained by considering a new on-site potential modified by the neighboring sites. For simplicity, let us consider just three spins, namely, ones on the sites -1, 0, and 1, where the site 0 corresponds to the center of the spin DB. In the weak-coupling limit, the dynamics of the neighboring spins at the sites ± 1 can be described by simple harmonic oscillation with a small amplitude ϵ, assuming the spin DB solution. From Eq. (5), we can obtain the following equation for the frequency of the spin precession at the site 0:

$$\tilde{\hbar}\omega s_0 = 2C s_0\sqrt{1 - \epsilon^2} + (2C\epsilon + s_0)\sqrt{1 - s_0^2}. \quad (8)$$

Considering $\epsilon \ll s_0 \lesssim 1$ in the weak-coupling limit, the above equation can be approximated to $\omega/\omega_m \approx 2C + \sqrt{1 - s_0^2}$, so that the new maximum frequency of local nonlinear oscillators, namely ω_m', is given by $\omega_m(2C+1)$, which means that the possible maximum frequency of a spin DB also increases under the coupling with the neighboring spins. Actually, this relation exactly coincides with the $k = \pi/2$ band edge of the spin wave as shown in Fig. 1 in the weak-coupling limit. Taking into account the instability caused by the resonance between DB's and phonons,[1] we should exclude the overlapping region between spin DB and the spin-wave band, so that finally the border of the existence of spin DB's is given by the $k = 0$ band edge, $\omega_m'/\omega_m = \sqrt{1 + 4C}$. The inset of Fig. 1 shows the amplitude of the spin oscillation at the central site
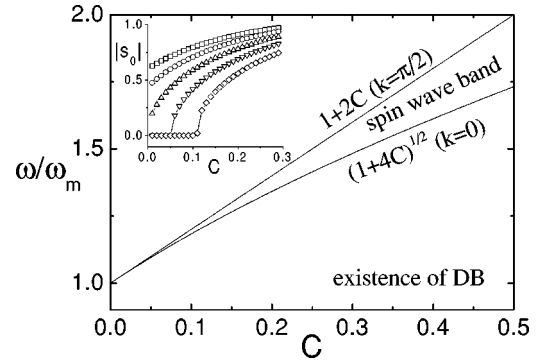

FIG. 1. The band structure of spin waves as a function of C. The inset represents the amplitude of the spin oscillation at the central site of spin DB as a function of C for a given frequency of spin DB ω_b, which is numerically obtained by using Eq. (5). From the upper part, they correspond to $\omega_b/\omega_m = 0.8$, 0.9, 1.0, 1.1, and 1.2, respectively.

of spin DB as a function of C for a given frequency of spin DB ω_b, where the criteria mentioned above can be also confirmed numerically. In other words, the frequencies of spin DB's are always located below the spin-wave band, which is nothing new in the sense of general criteria for the existence of a DB. We would like to mention, however, that this leads to somewhat interesting consequences that a spin DB appears above some critical coupling strength and disappears in the anticontinuous limit with the frequency of a spin DB fixed.[14] The mathematical proof for the existence of DB's was performed in this limit.[4]

Since Eq. (7) is Hamiltonian, M is symplectic, which implies that if λ is an eigenvalue, then λ^*, $1/\lambda$, and $1/\lambda^*$ are also eigenvalues. The linear stability of the DB solution requires that no eigenvalue must be outside unit circle. From both conditions, all eigenvalues are on the unit circle.[2] Figure 2 shows the evolution of the eigenvalues of the Floquet matrix M on unit circle (the angle ϕ of the eigenvalue $e^{i\phi}$) as a function of C for several ω_b's. For all calculations we take $\tilde{\hbar} = 1$. The angle ϕ has a simple relationship with the angular frequency ω through $\phi = 2\pi\omega/\omega_b$ [mod(2π)].[15] The continuous part of the Floquet spectrum corresponds to a spin-wave band, while $\phi = 0$ represents the spin DB itself. The
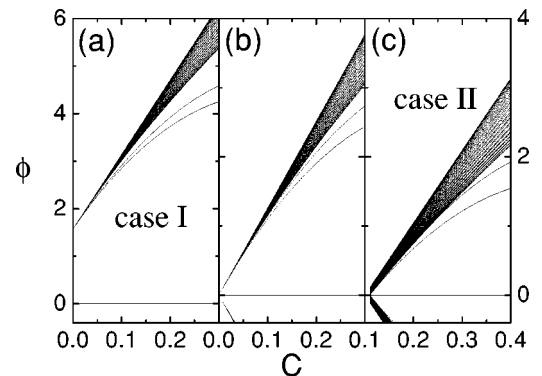

FIG. 2. Floquet spectrum obtained numerically for (a) $\omega_b/\omega_m = 0.8$, (b) $\omega_b/\omega_m = 1.0$, and (c) $\omega_b/\omega_m = 1.2$. See the left tick labels for (a) and the right tick labels for both (b) and (c).
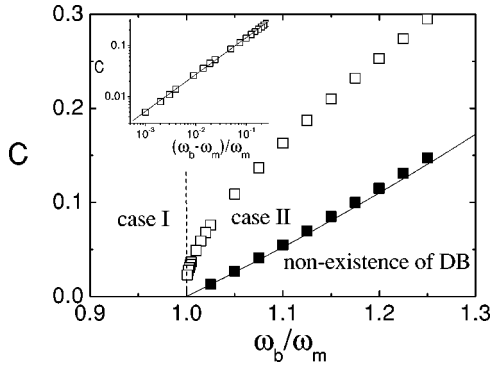
FIG. 3. The threshold of occurrences of symmetric (the filled squares) and antisymmetric (the open squares) ILE's as a function of the frequency of the spin DB obtained from numerically calculating Floquet spectra for various ω_b/ω_m. Spin DB's cannot exist in the region under the solid line (see the text for details). In the inset, we replot the threshold of the antisymmetric ILE's (the open squares) in log-log scale, which clearly shows power-law dependence.

eigenmodes detached from the bottom of the band are observed to be the ones that are localized. These are ILE's mentioned above. The ILE's belong to either symmetric or antisymmetric eigenmodes with respect to their reflection symmetry to the center of a spin DB. While for $\omega_b/\omega_m < 1$, two ILE's appear simultaneously at $C=0$ [Fig. 2(a)], for $\omega_b/\omega_m > 1$ at first the symmetric ILE appears at a certain value of C and then the antisymmetric one appears at larger C [Fig. 2(c)]. We call the former as case I and the latter as case II.

Figure 3 shows the threshold of the ILE's as a function of ω_b, where the dashed vertical line $\omega_b/\omega_m=1$, at which two spin-wave bands collide each other as shown in Fig. 2(b), divides the parameter space into two regions for the thresholds of ILE's (i.e., cases I and II). The solid line represents the border of the existence of spin DB's described by $C = [(\omega_b/\omega_m)^2 - 1]/4$ (the spin-wave band edge with $k=0$ in Fig. 1), below which the spin DB's cannot exist. It is mentioned that the threshold of the symmetric ILE (the filled squares) looks like a straight line, and that of the antisymmetric one (the open squares) shows the power-law dependence, namely, $C \propto \omega_b^{0.72}$ as shown in the inset of Fig. 3. This threshold behavior was also observed in the case of Klein-Gordon (KG) chain with ϕ^4 (double-well) on-site potential described by $V(x)=(x^4-2x^2)/4$,[16] where $\omega_b=2/3$, at which two neighboring phonon band edges with $k=0$ collide each other, plays a similar role as $\omega_b/\omega_m=1$ in our antiferromagnet. However, this frequency does not correspond to the maximum frequency of the local soft nonlinear oscillator, which is $\omega_m=1$ in a ϕ^4 KG chain. It should also be noted that in other KG chains with Morse ($V(x)=[1-\exp(-x)]^2/2$) or cubic [$V(x)=x^2/2-x^3/3$] on-site potential this is not the case, where for all $\omega_b (<\omega_m=1)$ the cubic and the Morse potentials correspond only to cases I and II, respectively. This has not been understood yet.

One of the reasons why we choose this magnetic lattice for our investigation is that experimentally the generation of a spin DB was reported in the quasi-1D biaxial antiferromag-
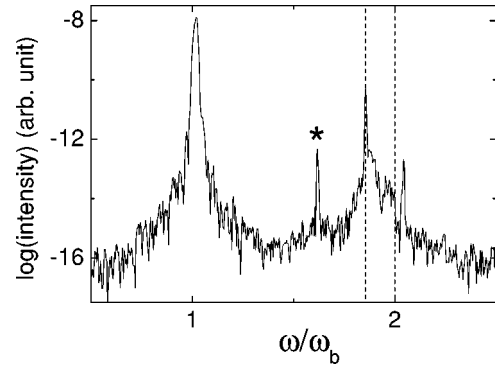
net $(C_2H_5NH_3)_2CuCl_4$ (Ref. 5), like the system studied in this paper. By microwave absorption experiment, the peak corresponding to the spin DB was observed in the spin-wave gap. The absorption spectrum measured in the experiment is proportional to the imaginary part of the dynamic magnetic susceptibility, which can be calculated using the Kubo expression.[5]

$$A(\omega) \propto \int_0^\infty dt \langle M^y(t+t')M^y(t') \rangle_{t'} e^{i\omega t}, \qquad (9)$$

where $M^y(t) = \sum_n s_n^y(t)$ and $\langle A \rangle_{t'}$ is the time average of the variable A. We calculate $M^y(t)$ using MD simulations with 103 spins starting from the solution of a spin DB obtained from Eq. (5) under the random amplitude noise.[17] Figure 4 clearly shows that an absorption peak, which is several orders of magnitude smaller than the spin DB peak, exists between the spin DB and the spin-wave band. Without noise we can obtain only the spin DB peak. Although the absorption power of this ILE is so tiny compared with that of the spin DB, it should not be ignored in comparison with that of the spin-wave band. It is worth noting that only the symmetric ILE can be observed in the absorption spectrum since the antisymmetric ILE disappears when the summation $\sum_n s_n^y(t)$ is performed. Figure 5 shows that the frequency of the symmetric ILE calculated using MD simulation is well fitted by the prediction of the linear theory in the region of small C. It is remarked that in the experiment of Ref. 5, somewhat broad spectrum of a spin DB was observed since many spin DB's with different frequencies were excited simultaneously. In order to observe the ILE's studied in this paper, more improved experimental status will be needed, for example, a single spin DB excitation, the suppression of volume and surface modes, better resolution in the absorption power, and so on. We also note that in general the antiferromagnetic ordering can persist only above some critical value of C, roughly speaking, of the order of 1. Even though it does not seem to be easy to find out experimentally the transition

FIG. 4. The power spectrum of $M^y(t)$ with $\omega_b/\omega_m=0.8$ and $C=0.3$. This is calculated using MD simulation with 103 spins during $256T_b$ ($T_b=2\pi/\omega_b$) under the random noise with the intensity $D=10^{-5}$ (Ref. 14). "$\star$" indicates the symmetric ILE, above which the spin-wave excitations are shown. The vertical dashed lines represent the upper and the lower spin-wave band edges obtained from the dispersion relation.
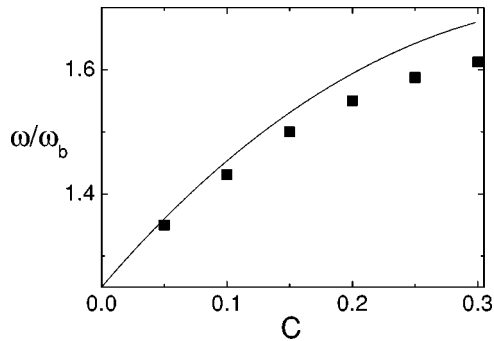
FIG. 5. The frequency of the symmetric ILE given by the Floquet spectrum in Fig. 2(a) (the solid curve) and by the power spectrum of $M^y(t)$ using MD simulation (the filled square).

from case I to II in this system, due to this reason, it is still possible to observe the ILE's themselves for higher values of C.

In our previous work on discrete nonlinear Schrödinger (DNLS) equation[10] we already noted that the DNLS equation is the nontrivial simplest system for studying scattering problems or ILE's. However, it has only a single parameter since the change of the breather frequency ω_b can be compensated by scaling $\Omega \rightarrow \Omega/\omega_b$ and $C \rightarrow C/\omega_b$, where Ω and C are the frequencies of the small perturbation and the linear coupling strength, respectively. We would like to point out that the 1D antiferromagnet with easy-axis anisotropy provides a good intermediate example with two spin-wave bands (or scattering channels) and two parameters (C and ω_b) between the case of DNLS equation with two phonon bands and one parameter (C/ω_b), and that of the KG chain with an infinite number of phonon bands and two parameters.

In summary, we have investigated the characteristics and the possibility of experimental observation of the ILE's in 1D antiferromagnets with easy-axis anisotropy using both linear analyses and MD simulations. The structure of the thresholds of the ILE's strongly depends on the frequency of a spin DB. For $\omega_b/\omega_m < 1$, the ILE's appear at $C=0$ simultaneously, while for $\omega_b/\omega_m > 1$ the symmetric ILE occurs at first at a certain value of C and then the antisymmetric one appears at a larger value of C. It is shown that the frequency of the ILE's calculated using MD simulation is well fitted by the prediction of the linear theory. We hope that these ILE's will be observed in experiments.

[1] S. Flach and C.R. Willis, Phys. Rep. **295**, 181 (1998).

[2] S. Aubry, Physica D **103**, 201 (1997).

[3] A.J. Sievers and S. Takeno, Phys. Rev. Lett. **61**, 970 (1988).

[4] R.S. Mackay and S. Aubry, Nonlinearity **7**, 16 233 (1991).

[5] U.T. Schwarz, L.Q. English, and A.J. Sievers, Phys. Rev. Lett. **83**, 223 (1999).

[6] P. Binder, D. Abraimov, A.V. Ustinov, S. Flach, and Y. Zolotaryuk, Phys. Rev. Lett. **84**, 745 (2000).

[7] R. Lai and A.J. Sievers, Phys. Rep. **314**, 147 (1999).

[8] Y. Zolotaryuk, S. Flach, and V. Fleurov, Phys. Rev. B **63**, 214422 (2001).

[9] S. Kim, C. Baesens, and R.S. Mackay, Phys. Rev. E **56**, R4955 (1997).

[10] S.W. Kim and S. Kim, Physica D **141**, 91 (2000).

[11] S. Lee and S. Kim, Int. J. Mod. Phys. B **14**, 1903 (2000).

[12] S.W. Kim and S. Kim, Phys. Rev. B **63**, 212301 (2001).

[13] R. Lai, S.A. Kiselev, and A.J. Sievers, Phys. Rev. B **54**, R12 665 (1996).

[14] S. Neusüß and R. Schilling, Phys. Rev. E **60**, 6128 (1999).

[15] T. Cretegny, S. Aubry, and S. Flach, Physica D **119**, 73 (1998).

[16] S. Kim and R. S. Mackay (unpublished).

[17] At each time step of numerical integrations of Eq. (4), we add random amplitude noises $D\xi_n$ to the variables s_n, where the absolute values of ξ_n are normalized to 1, and D represents the strength of noise. $T_b/1024$ ($T_b = 2\pi/\omega_b$) is used as the time interval for numerical integration.